



Inhibition of Plk1 induces mitotic infidelity and embryonic growth defects in developing zebrafish embryos

KilHun Jeong¹, Jae-Yeon Jeong¹, Hae-Ock Lee², Eunhee Choi, Hyunsook Lee^{*}

Department of Biological Sciences and Institute of Molecular Biology and Genetics, College of Natural Sciences, Seoul National University, 599, Gwanak-Ro, Gwanak-Gu, Seoul 151-742, Korea

ARTICLE INFO

Article history:

Received for publication 15 December 2009
Revised 29 May 2010
Accepted 1 June 2010
Available online 8 June 2010

Keywords:

Zebrafish embryo
Plk1
Live-imaging
Prometaphase
Mitosis
BI 2536

ABSTRACT

Polo-like kinase 1 (Plk1) is central to cell division. Here, we report that Plk1 is critical for mitosis in the embryonic development of zebrafish. Using a combination of several cell biology tools, including single-cell live imaging applied to whole embryos, we show that Plk1 is essential for progression into mitosis during embryonic development. Plk1 morphant cells displayed mitotic infidelity, such as abnormal centrosomes, irregular spindle assembly, hypercondensed chromosomes, and a failure of chromosome arm separation. Consequently, depletion of Plk1 resulted in mitotic arrest and finally death by 6 days post-fertilization. In comparison, Plk2 or Plk3 morphant embryos did not display any significant abnormalities. Treatment of embryos with the Plk1 inhibitor, BI 2536, caused a block in mitosis, which was more severe when used to treat *plk1* morphants. Finally, using an assay to rescue the Plk1 morphant phenotype, we found that the kinase domain and PBD domains are both necessary for Plk1 function in zebrafish development. Our studies demonstrate that Plk1 is required for embryonic proliferation because its activity is crucial for mitotic integrity. Furthermore, our study suggests that zebrafish will be an efficient and economical in vivo system for the validation of anti-mitotic drugs.

© 2010 Elsevier Inc. All rights reserved.

Introduction

Exquisite mechanisms to preserve the integrity of the genome exist at every step of the cell division process. Progression of mitosis and cytokinesis must be precisely coordinated for accurate cell division. Polo-like kinase 1 (Plk1), a conserved Polo family serine/threonine kinase, has multifaceted roles in mitotic entry, progression, exit, and cytokinesis (Barr et al., 2004; Petronczki et al., 2008). Consistent with its broad range of functions, Plk1 localizes to each significant mitotic structure as cells progress through cell division: the centrosomes and kinetochores from prophase to metaphase, the central spindle in anaphase, and the spindle midzone in telophase (Barr et al., 2004).

Yeast possess a single Polo kinase, whereas metazoans possess at least two Polo-like kinases: *Drosophila* expresses *Polo* and *Plk4* (also known as *SAK*) and mammals express four members of the Plk family (*Plk1*, *Plk2*, *Plk3*, and *Plk4*) (Archambault and Glover, 2009). In all Plks, carboxy-terminal Polo box domain (PBD) follows the Ser/Thr kinase domain. However, Plk1, Plk2, and Plk3 are structurally related in that they possess two Polo boxes, which are required to form binding

pockets for phosphorylated motifs in target proteins (Cheng et al., 2003; Elia et al., 2003a,b). Of the three resembling Plks, reports suggest that it is Plk1 that exerts most of its mitotic functions in mammals (Petronczki et al., 2008). Meanwhile, the functions of Plk2 and Plk3 are much less understood. However, Plk2 and Plk3 have been suggested to function in interphase (Archambault and Glover, 2009).

Unlike others, Plk4 has a single Polo box and is distinct from other family members. How the PBD domain of Plk4 recognizes its substrates is not yet understood (Archambault and Glover, 2009). In *Drosophila* and humans, Plk4 is specifically and completely required for centriole duplication (Bettencourt-Dias et al., 2005; Habadanck et al., 2005). However, mice haploinsufficient in the *Plk4* allele exhibit mitotic infidelity and tumorigenesis, implicating Plk4 in cell division (Ko et al., 2005). Taken together, it seems that the different Plks exert both overlapping and distinct functions. The detailed mechanism how different members of the Plk family are coordinated in vivo is not yet fully established.

The function of Plk1 in the cell division cycle has been most extensively studied in cell culture systems. However, the results are complicated and controversial between transformed and non-transformed cells: depletion of Plk1 activity results in mitotic arrest in HeLa cells, but in G2 arrest in normal fibroblasts (Lane and Nigg, 1996). Inhibition of Plk1 in cancer cells induces apoptosis after a mitotic delay (Gumireddy et al., 2005; Steegmaier et al., 2007), while non-transformed cells survive Plk1 depletion (Liu et al., 2006).

^{*} Corresponding author.

E-mail address: HL212@snu.ac.kr (H. Lee).

¹ These authors contributed equally.

² Current address: Department of pathology, Korea University, College of Medicine, Korea University, Seoul, Korea.

Model organisms have provided critical clues about the functions of Plk1 in cell division. Mutations in Plk1 orthologues in *Drosophila* and yeasts result in mitotic arrest due to aberrant mitotic chromosome arrangements and abnormal spindle poles. These mutations also lead to polyploid and aneuploid cells (Hartwell and Smith, 1985; Lamazares et al., 1991; Ohkura et al., 1995; Sunkel and Glover, 1988). In *Xenopus*, immunodepletion of Plx1, the orthologue of Plk1, in early embryos results in the cleavage arrest that is associated with monopolar spindles (Qian et al., 1998). As Plx1 is required for the activation of Cdc25C and Cdk1-cyclinB (Qian et al., 2001), these results indicate that *Xenopus* Plk1 is required at multiple points in mitosis. Plk1-deficient mice exhibit early embryonic lethality around the eight-cell stage; however, the heterozygous mice survive to adulthood and display increased tumor incidence (Lu et al., 2008). Taking these into account, it occurred to us that studying *Plk1* in zebrafish might help reveal its *in vivo* functions. Utilizing single cell live-imaging techniques and cell biological assays in whole embryos, we show the critical roles of zebrafish Plk1 in the homeostasis of mitotic chromosomes, centrosomes, and microtubule spindles in embryogenesis. The expression level and kinase activity of Plk1 were crucial for embryonic growth and development; either increased or decreased Plk1 levels led to chromosome instability. In comparison, two other related Plk kinases, *Plk2* and *Plk3*, were dispensable for zebrafish embryogenesis. By soaking the developing embryos in egg water treated with the Plk1 inhibitor BI 2536, we confirmed that the drug is specific to Plk1 in zebrafish embryos; BI 2536-treated embryos formed monopolar spindles and were completely blocked in mitosis, followed by frequent cell death or premature exit from mitosis. Taken together, these results suggest that Plk1 is essential in mitosis and, therefore, is critically required for embryonic development. We also demonstrate that zebrafish embryogenesis is an excellent *in vivo* model system for assessing mitotic functions and validating the efficiencies of mitotic kinase inhibitors.

Materials and methods

Zebrafish

Wild-type zebrafish were purchased from a local fish store. Embryos were obtained through natural spawning and were raised at 28.5 °C, injected, and staged, according to standard procedures (Kimmel et al., 1995).

Cloning of zebrafish *plk1*, *Plk2*, *Plk3*, and *Mad1*

Zebrafish *Plk1*, *Plk2*, *Plk3*, and *Mad1* cDNAs were cloned by RT-PCR, based on the published mRNA sequences (*Plk1*, GenBank accession number NM_001003890; *Plk2*, NM_001099245; *Plk3*, NM_201308; *Mad1*, EMBL accession number BX927386.11). The cloned sequences matched with the public databases with small variations: the *Plk1* clone has an allelic variation that substitutes glutamate for lysine at residue 340 in NP_001003890; the *Mad1* clone has Lysine and Proline inserted in-frame before Glutamine at residue 329 in BX927386.11. All of the sequences have been submitted to GenBank.

In situ hybridization

An antisense RNA probe for *Plk1* was synthesized using SP6 RNA polymerase in the presence of DIG RNA labeling mix (Roche), and *in situ* hybridization was performed, as described (Jeong et al., 2006).

Injection of morpholinos (MOs) and sense RNAs

Translation-blocking *plk1* ATG MO (5'-AATGCAGCACTCATCGTTGTACAC-3'), splice-blocking *plk1* sMO (5'-GCTTCCAGCTCTTACCTTCTGC-3'), splice-blocking *plk2* sMO (5'-TATGCAGTGTATCTACCTTCTC-3'),

splice-blocking *plk3* sMO (5'-TCTTGGTTGAAACAACCTCACCT-3') were all designed and purchased from GeneTools (Philomath, OR). For RNA injection, *Plk1* and *Mad1* cDNAs were subcloned into pCS2-EGFP and *in vitro* transcribed. Mutations in *Plk1* were generated by site-directed mutagenesis. Sense RNA was synthesized using the mMessage mMachine kit (Ambion, Austin, TX). *Plk1* RNA at (1 nl of 750 ng/μl) and *Mad1* RNA (1 nl of 1400 ng/μl), respectively, were injected into the yolk of one-cell stage embryos.

Western blotting

Whole embryos were lysed in 3X SDS-PAGE sample loading buffer and equal volumes of lysate were analyzed at each stage using a mouse anti-Plk1 antibody cocktail (Zymed Laboratories, 1:250).

Antibodies and Immunofluorescence assays in whole embryos

The following antibodies were used for immunohistochemistry and immunofluorescence microscopy: rabbit anti-phosphohistone H3 (Ser10) antibody (pH3, Millipore, Billerica, MA, 1:1,000); mouse anti-α-tubulin antibody (Sigma, 1:500); mouse and rabbit anti-γ-tubulin antibody (Sigma, 1:1,000). Alexa fluor-conjugated secondary antibodies (Molecular Probes) and biotin-conjugated secondary antibodies (Vector Laboratories, Burlingame, CA) were diluted at 1:1,000 for immunostaining.

In immunostaining experiments with anti-α-tubulin, anti-γ-tubulin, and anti-pH3 antibodies, fluorescence microscopy was performed after the embryos were fixed in 4% paraformaldehyde, washed three times in PBS containing 0.1% Triton X-100 (PBT), and rehydrated by serial washing with 50% PBT/methanol, 75% PBT/methanol, and then 100% PBT. The embryos were treated with cold acetone for 7 min at −20 °C and then washed twice with PBT. Finally, the embryos were washed in PBS containing 1% DMSO, 0.05% Triton X-100, and 0.01% Tween 20 (PBDTT). Fixed embryos were incubated in blocking buffer (1% BSA, 10% goat serum in PBDTT) for 1 h. Primary and secondary antibodies were incubated in the blocking solution, washed, and finally mounted in Vectashield containing DAPI (Vector Laboratories). Images of cells at the surface of the yolk or at the end of the tail were taken and processed with DeltaVision (AppliedPrecision, WA) (Choi et al., 2009). Optical sections (1 μm) of 14 images were obtained, processed, and deconvolved using the SoftWarx program.

Metaphase chromosome spreads of zebrafish embryos

Metaphase chromosome spreads were performed according to the published protocol for cultured MEFs (Lee et al., 1999), with modifications to optimize for zebrafish embryos. Prometaphase arrest was induced by treating embryos with 400 ng/ml nocodazole for 2 h at 24 hpf in control embryos. Yolks were dissected away from the embryos in 1.1% sodium citrate for 8 min at room temperature, and embryos were transferred to new 1.1% sodium citrate and incubated for 8 min on ice. The embryos were then incubated in a methanol/acetate solution (3:1) for 20 min on ice and then at −20 °C overnight. Each embryo was then minced with forceps in 50% acetic acid and dropped on slides, dried, and counterstained with DAPI. Images were taken on a Zeiss Axio Observer Z1 microscope with a 100× objective.

Time course measurement of mitotic entry and mitotic exit

5-bromo-2-deoxyuridine (BrdU) labeling was performed, as previously described (Lee and Kimelman, 2002) in 24 hpf embryos of control and *Plk1* morphants. After 30 min of BrdU incorporation, embryos were washed and incubated in egg water for 2h intervals for up to 10 h, as indicated. The labeled embryos were then fixed in paraformaldehyde, and subjected to double immunostaining with anti-BrdU- and anti-pH3 antibodies. Mitotic cells (pH3-positive) with

BrdU were counted and recorded as percentage of total cells at each indicated time point.

Apoptosis assay

For TUNEL staining, embryos were fixed in 4% paraformaldehyde, permeabilized in methanol, digested in proteinase K (5 µg/ml) for 5 min, fixed in 4% paraformaldehyde for 20 min, and then incubated with 20 units of terminal deoxynucleotidyl transferase and 1.3 µM of DIG-11dUTP (Roche Applied Science) for 4 h at room temperature. Embryos were washed twice in a buffer containing 50% formamide, 2X SSC, and 0.1% Tween-20 for 15 min at 55 °C and then in PBS containing 0.1% Tween-20. Apoptotic cells were visualized with alkaline phosphatase-conjugated anti-DIG antibodies (Roche) and NBT/BCIP.

MPM-2 staining and flow cytometry

Zebrafish embryos were dechorinated manually and washed twice in PBS. Embryos were then meshed between two slides, and the dispersed cells were washed once in PBS and passed through a 100-µm cell strainer. Single cells were fixed in 70% ethanol at –20 °C. The cells were then subjected to MPM-2 immunostaining, followed by propidium iodide staining before analysis in flow cytometry. Flow cytometry was performed using a FACSCanto™ II flow cytometer (Becton Dickinson), as with cultured cells (Choi et al., 2009).

Analysis of the spindle assembly checkpoint activation by *Mad1* localization

One picomole of control or *Plk1* morpholino oligos were injected into one- to four-cell stage embryos with RNA expressing *GFP-Mad1* (1.4 ng/embryo). At 24 hpf, zebrafish embryos (> 15 embryos) were dechorinated and manually dissociated, as described above. For controls, embryos were treated with 200 ng/ml of nocodazole for 2 h, washed in PBS, and dissociated. Cells were then centrifuged at 1200 rpm for 5 min at RT in a Cytospin (Shadon Cytospin4, Thermo Scientific). After fixation in 4% paraformaldehyde, cells were counterstained with DAPI, and the images were processed and analyzed for GFP-fluorescence with chromosomes on a DeltaVision RT.

Generation of H2B-GFP transgenic zebrafish

A transgenic line of zebrafish expressing zebrafish H2B (NM_200117) fused to GFP was generated using the Tol2 transposable element system (pT2AL200R150G and pCS-TP) (Urasaki et al., 2006). GFP-positive embryos were examined for mitotic timing and chromosome segregation using time-lapse video microscopy. The embryos with normal mitotic timing (NEBD to anaphase around 16 min without mitotic infidelity) were selected and allowed to mature to adulthood.

Time-lapse microscopy of live embryos

H2B-GFP transgenic fish were crossed with wild-type fish and the embryos were injected with either the control MO or *plk1* ATG MO at the one- to four-cell stages. Embryos were allowed to grow at 28.5 °C and the GFP-positive embryos were manually dechorinated. In

experiments where BI 2536 treatment was used, the drug was added at 22 hpf followed by 2 h incubation at 28.5 °C. Embryos were then placed in 0.3% low melting agarose containing 150 µg/ml tricaine. Time-lapse microscopy was done on a DeltaVision. Optical sections (2 µm) of three consecutive images were collected every 2.5 min at 28.5 °C and merged.

In vitro kinase assay

Zebrafish *Plk1*, *Plk2*, and *Plk3* cDNAs were cloned by RT-PCR from zebrafish embryos and subcloning into pGEX 4 T-1. They were expressed and purified as GST- fusion proteins from *Escherichia coli*. In vitro kinase assays for *Plk1*, *Plk2*, and *Plk3* were performed in the absence or presence of BI 2536 (100 µM). In each reaction, 100 ng of recombinant kinases were tested for kinase activity towards 10 µg of Casein protein (Sigma) in a total volume of 30 µl of reaction buffer (10 mM Tris at pH 7.5, 10 µM sodium vanadate, 10 mM MgCl₂, 10 µM ATP, 1 mM DTT, 5 µCi [γ -³²P]ATP [3000 Ci/mmol, 10 mCi/mL]) at 30 °C. Reactions were stopped after 30 min by the addition of sample buffer. Samples were resolved by SDS-PAGE and visualized by autoradiography.

Results

Expression of *plk1* in the proliferating regions of zebrafish embryos

To study the role of *Plk1* in zebrafish embryogenesis, we first cloned zebrafish *Plk1* by RT-PCR. The amino acid sequence of zebrafish *Plk1* was 72.1% identical to that of human *Plk1*. Importantly, the kinase domain, D-box, PBD 1, and PBD 2, all of which are important for *Plk1* function, were well conserved across species (Fig. 1A).

We next performed *in situ* hybridization to assess the expression patterns of *Plk1*. *Plk1* was expressed both maternally and zygotically (Fig. 1B). The expression of *Plk1* mRNA was ubiquitous by the bud stage, but became restricted to the proliferating tissues, such as brain, eyes, spinal cord, somites, fin folds, and tail bud, by 24 h post fertilization (hpf) (Fig. 1B).

To understand the role of *Plk1* in zebrafish development, knockdown of *Plk1* expression was performed by injecting morpholino oligos (MO) that block translation initiation (ATG MO) or splicing between exon 1 and intron 1 of *plk1* (sMO). Two different MOs were injected into the yolk of one- to four-cell stage embryos, and the efficiency and specificity of these *plk1* MOs was assessed by immunoblotting zebrafish embryo lysates from 26 hpf with an anti-*Plk1* antibody cocktail. Injection of *plk1* ATG MO and sMO at 0.5 pmol/embryo and 0.25 pmol/embryo, respectively, reduced *Plk1* expression to ~80% compared to the injection of control MO at 1 pmol/embryo (Fig. 1C).

Next, we analyzed the effects of the *plk1* MOs at various developmental stages. We found that injection of 0.5 pmol of *plk1* ATG MO decreased *Plk1* levels by 26% at the bud stage, 74% at the 10-somite stage, 77% at the 20-somite stage, and 79% at 24 hpf (Fig. 1D). These results demonstrate that the activity of the *plk1* MO was gradual and most effective after gastrulation, probably due to the presence of maternal *Plk1*. Because the phenotypes after injection of *plk1* ATG MO and sMO were similar in all experiments, we present here the results obtained with *plk1* ATG MO.

Fig. 1. Expression and morpholino-induced knockdown of *Plk1* in zebrafish embryos. (A) Alignment of the ATP-binding pockets, D-boxes, and polo-box domains of *Plk1* sequences from zebrafish and other species. Amino acid sequences were aligned using Clustal W. Conserved amino acids are highlighted in yellow. Asterisks indicate the mutated residues used in Fig. 7. (B) Analysis of *plk1* expression by *in situ* hybridization in wild-type zebrafish embryos at various developmental stages: hb, hindbrain; mhbm, midbrain-hindbrain boundary; sc, spinal cord; tec, tectum. (C) Embryos were injected with the indicated amounts of control MO, *plk1* ATG MO, or *plk1* sMO in the yolk. Whole embryo lysates were prepared at 26 hpf and subjected to western blot analysis (WB) with anti-human *Plk1* antibody. The slower migrating band is a non-specific band (ns). (D) Embryos were injected with 0.5 pmol of control (CM) or *plk1* ATG MO (PM), and the whole embryo lysates were subjected to WB with anti-*Plk1* antibodies. The same blot was reprobed with anti- β -actin antibodies for a loading control.

Depletion of *Plk1* expression results in growth defects and cell death during zebrafish development

To assess the effects of *Plk1* knockdown during embryonic development, embryos injected with various concentrations of *plk1* MO (0.25 to 1 pmol) were observed and photographed at different developmental stages. Consistent with the high level of *Plk1* expression that accumulated by the bud stage, *plk1* MO did not interfere with the embryonic development before the end of gastrulation (data not shown). In contrast to the absence of a phenotype before gastrulation in *plk1* morphants, mice deficient in a *Plk1* allele exhibit early embryonic lethality (Lu et al., 2008). We speculated that the presence of maternal *Plk1* protein, which was expressed from the abundant maternal transcripts, enabled the zebrafish morphants to survive beyond gastrulation. This result demonstrates that the zebrafish *plk1* morphants provide advantages for assessing the roles of *Plk1* in vertebrate development.

Later in development, *Plk1* morphants at 24 and 48 hpf displayed growth defects: smaller body and tissue sizes compared to the control morphants; fragile epidermis; and loosely organized tissues. These defects became more severe with increasing doses of morpholino (Fig. 2A).

When injected with 0.5 pmol of *plk1* MO, *plk1* morphants survived until 4 days post fertilization (dpf) with growth defects (86%, $n = 49$) and then died by 6 dpf (100%, $n = 50$). In contrast, 94% of the embryos injected with 0.5 pmol of control MO survived to 6 dpf without any signs of abnormality ($n = 50$).

To examine whether *plk1* knockdown induces apoptosis, control and *plk1* morphants were collected at 28 hpf and subjected to TUNEL staining. We found that apoptotic cell death was markedly increased in the *plk1* morphants, particularly in proliferating tissues, such as the spinal cord, fin folds, and tail bud (Fig. 2B). Collectively, *Plk1* knockdown by MO injection resulted in impaired embryonic growth and apoptosis.

Knockdown expression of *Plk1* results in prometaphase arrest

Next, we analyzed the molecular basis for embryonic growth failure in *plk1* morphants. Because *Plk1* participates in mitosis in other species, we asked if *Plk1* depletion affected the mitotic cell cycle. After being injected with *plk1* MO, 24 hpf embryos were fixed and immunostained with anti-phosphohistone H3 (pH3) antibody (Giet and Glover, 2001; Hsu et al., 2000). We observed that *Plk1* knockdown resulted in a dramatic increase of pH3-positive cells throughout the embryonic body (Fig. 2C), indicating the accumulation of mitotic cells in *plk1* morphant embryos that were defective in growth.

To determine if defects in mitosis existed, we adopted the BrdU pulse-chase experiment in combination with the anti-BrdU and anti-pH3 co-immunofluorescence assays (Shepard et al., 2007; Shepard et al., 2005). In controls, BrdU-positive mitotic cells (cells positive for both BrdU and pH3) dramatically increased 2 h post BrdU incorporation and dropped at 6 h post-pulse. The result indicates that G2/M transition and mitotic entry took place at/around 2 h post-pulse and exit from mitosis took place at/around 6 h in control embryos. In *plk1* morphant embryos, mitotic entry began at/around 2 h, similar to the control. However, exit from mitosis was detected around 10 h (Fig. 2D). These results suggest that the *plk1* morphant cells are capable of entering into mitosis, but are then delayed in mitosis. This mitotic delay may have resulted in embryonic growth failure.

Mitotic delay is primarily governed by the metaphase-anaphase transition by the spindle assembly checkpoint (SAC), which inhibits APC/C until all chromosomes achieve bipolar spindle attachment (Nasmyth, 2005; Peters, 2006). Therefore, we asked whether *Plk1* depletion resulted in SAC activation. It has been reported that *Plk1* is critical for stable kinetochore-spindle attachments in cultured cells (Elowe et al., 2007) and that the treatment of HeLa cells with *Plk1*

inhibitors results in SAC activation (Lenart et al., 2007). To assess for the SAC activation, we isolated cells from control and *plk1* morphants at 28 hpf and subjected them to MPM2 immunostaining (Lee et al., 1999). MPM-2 is a monoclonal antibody that is specific to mitotic cells (Davis et al., 1983). In the event of SAC activation, such as due to prolonged treatment with microtubule poisons, MPM-2 staining increases dramatically over time. Thus, it occurred to us that the index of MPM-2 staining would be a useful assessment of SAC activation (Choi et al., 2009; Lee et al., 1999) in this setting. The result showed that the number of cells immunostained with MPM-2 after DNA replication was dramatically increased in *plk1* morphants (43.2%), compared to control (1.8%), supporting the idea that *plk1* morphant cells are delayed in mitosis (Fig. 2E). Interestingly, *plk1* morphants produced two distinct mitotic populations; 33.8% of the cells displayed normal 4 N DNA and 9.4% of the cells exhibited 8 N DNA content, indicating the presence of polyploid cells (Fig. 2E).

As a second assessment of SAC activation in *plk1* morphants, we scored and compared the numbers of prometaphase cells with Mad1 localized at the kinetochores. Mad1 is a component of the SAC (Hardwick and Murray, 1995) and is required for Mad2 to localize to kinetochores (Chung and Chen, 2002; Sironi et al., 2001). Because the antibodies to Mad1 or Mad2 did not work in zebrafish embryos, we cloned zebrafish *Mad1* and linked it to GFP at the C-terminus, in vitro transcribed, and co-injected the RNA into one- to four-cell embryos with control or *plk1* MO. In controls, less than 2% of cells were at prometaphase where Mad1 was at the kinetochores (1.25%, $n = 672$). Nocodazole treatment increased the numbers of Mad1-localized prometaphase cells (4.7%, $n = 1072$). Notably, *Plk1* depletion resulted in a marked increase of Mad1-localized prometaphase cells (17.6%, $n = 798$), supporting that SAC is activated upon *Plk1* depletion (Fig. 2F). We were aware of the report that Mad1 phosphorylation by *Plk1* was required for Mad1 and Mad2 to localize to kinetochores in cultured cells (Chi et al., 2008). However, in zebrafish embryos, the degree of Mad1 localized to kinetochores was not affected by the depletion of *Plk1* (Fig. 2G). Taken together, we suggest that *Plk1* depletion during zebrafish embryogenesis led to SAC activation and prometaphase arrest, resulting in growth defects.

Next, to closely examine the causes of the mitotic arrest associated with *Plk1* depletion, embryos were assayed for microtubule organization in relation to chromosomes by co-immunostaining with antibodies against pH3 and α -tubulin. Tails from three embryos of each group were cut and analyzed by fluorescence microscopy to assess the mitotic phase, chromosome integrity, and spindle assembly (Fig. 2H and supplemental Fig. S2). Compared to cells derived from control morphants, *plk1* morphant cells displayed a marked increase in prometaphase cells, as shown by the patterns of microtubule spindles in relation to the pH3-positive chromosomes (Fig. 2H, *plk1* MO). Furthermore, none of the *plk1* morphant cells analyzed had entered anaphase, confirming that *Plk1* knockdown led to delay in mitosis (Fig. 3A).

Knockdown of *Plk1* leads to centrosome defects, congression errors, and impaired spindle assembly

Plk1 has been implicated in the centrosome-maturation checkpoint in cultured cells (Lane and Nigg, 1996). Indeed, immunostaining of the embryos with antibodies against α -tubulin and γ -tubulin revealed centrosome defects in *plk1* morphants. Mitotic cells in the controls displayed well-separated centrosomes at opposite poles (Fig. 3Ba). By comparison, knockdown of *Plk1* frequently resulted in a lack of γ -tubulin staining in one pole, while the opposite pole was composed of two γ -tubulin-positive centrosomes in the same focal plane (Fig. 3Bb). Monopolar spindles with circular chromosome arrangements, which are indicative of a centrosome separation failure, were also observed (5.5%, $n = 3$) (Fig. 3Bc). A number of *Plk1*-deficient cells displayed disorganized spindles with centrosomes

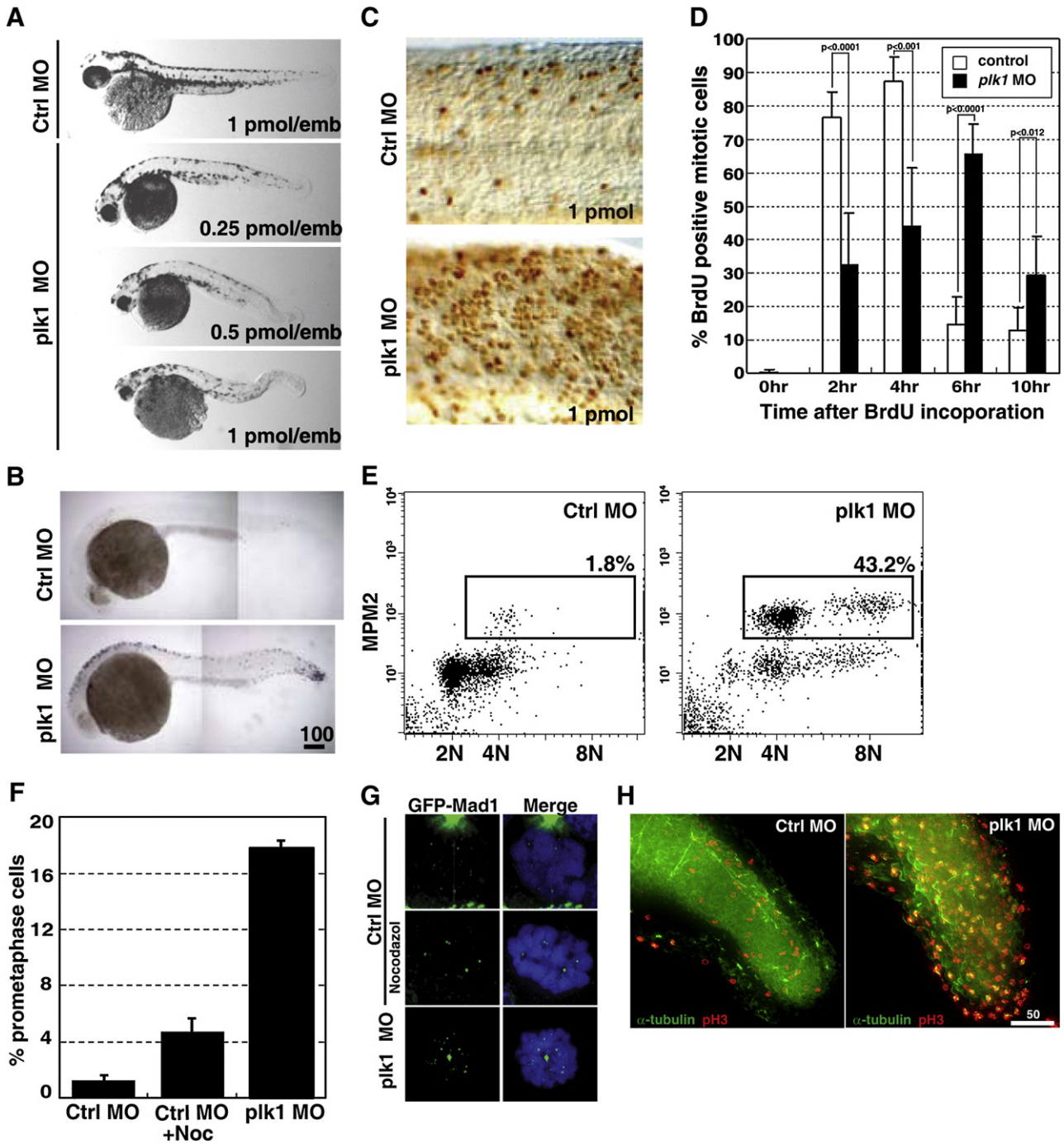


Fig. 2. Depletion of *Plk1* expression results in growth failure and apoptosis due to activation of SAC. (A) Zebrafish embryos were injected with various concentrations of control (Ctrl) or *plk1* ATG MO (*Plk1* MO) at the one- to four-cell stages. Photographs were taken at 48 hpf. (B) Embryos were injected with 0.5 pmol of control or *plk1* ATG MO, and apoptosis was assayed by TUNEL staining at 28 hpf. Apoptotic cells are shown as purple dots. (C) Embryos were injected with 1 pmol of control or *plk1* ATG MO and stained with anti-phosphohistone H3, Ser10 (pH3) antibodies at 24 hpf. (D) Time course from S phase into/out of G2/M, as shown by BrdU incorporation followed by double pH3/BrdU staining at indicated time points post BrdU pulse. Embryos injected with 0.25 pmol of control or *plk1* ATG MO are compared. The percentage of BrdU/pH3 double-positive cells are represented in bar graphs (mean \pm s.e.m.; $n \geq 385$ cells from 2 embryos each). (E) MPM-2 staining for mitotic index measurement. X-axis, 7AAD for DNA staining; Y-axis, MPM-2 staining. (F) Comparison of the percentage of cells with GFP-Mad1 at the prometaphase kinetochores in control, nocodazole-treated, and *plk1* MO-injected embryos. The results are the average of two independent experiments. At least 15 embryos each were analyzed in each experiment. (G) Localization of Mad1 at the prometaphase kinetochores in control, nocodazole-treated, and *plk1* MO-injected embryos. The results are the average of two independent experiments. (H) Embryos injected with 0.5 pmol of control or *plk1* ATG MO were subjected to co-staining with anti- α -tubulin and anti-pH3 antibodies at 24 hpf. Optical sections were acquired every 1 μ m at the end of the tails, merged and deconvoluted. Green, α -tubulin; red, pH3. Scale bar, 50 μ m. Enlarged images are presented in Supplemental Fig. S2.

of apparently different sizes, demonstrating defective centrosome maturation (Fig. 3Bd and e). Multipolar spindles with disorganized chromosomes were also observed (51.5%, $n=28$) (Fig. 3Be). In addition to defects in centrosome maturation, a failure of chromosome congression was observed in *Plk1*-deficient cells (27%, $n=15$) (arrows in Fig. 3Bb–d). Close examination of the results in Fig. 2H

(supplemental Fig. S2) at the single cell level confirmed the failure of chromosome congression in cells of *Plk1* morphants, as well as irregular microtubule spindles (Fig. 3Cb–f). Collectively, zebrafish *Plk1* is required for chromosome congression, centrosome maturation, and regulation of microtubule spindle outgrowth. Defects in all of these functions cause problems in bipolar spindle attachment to

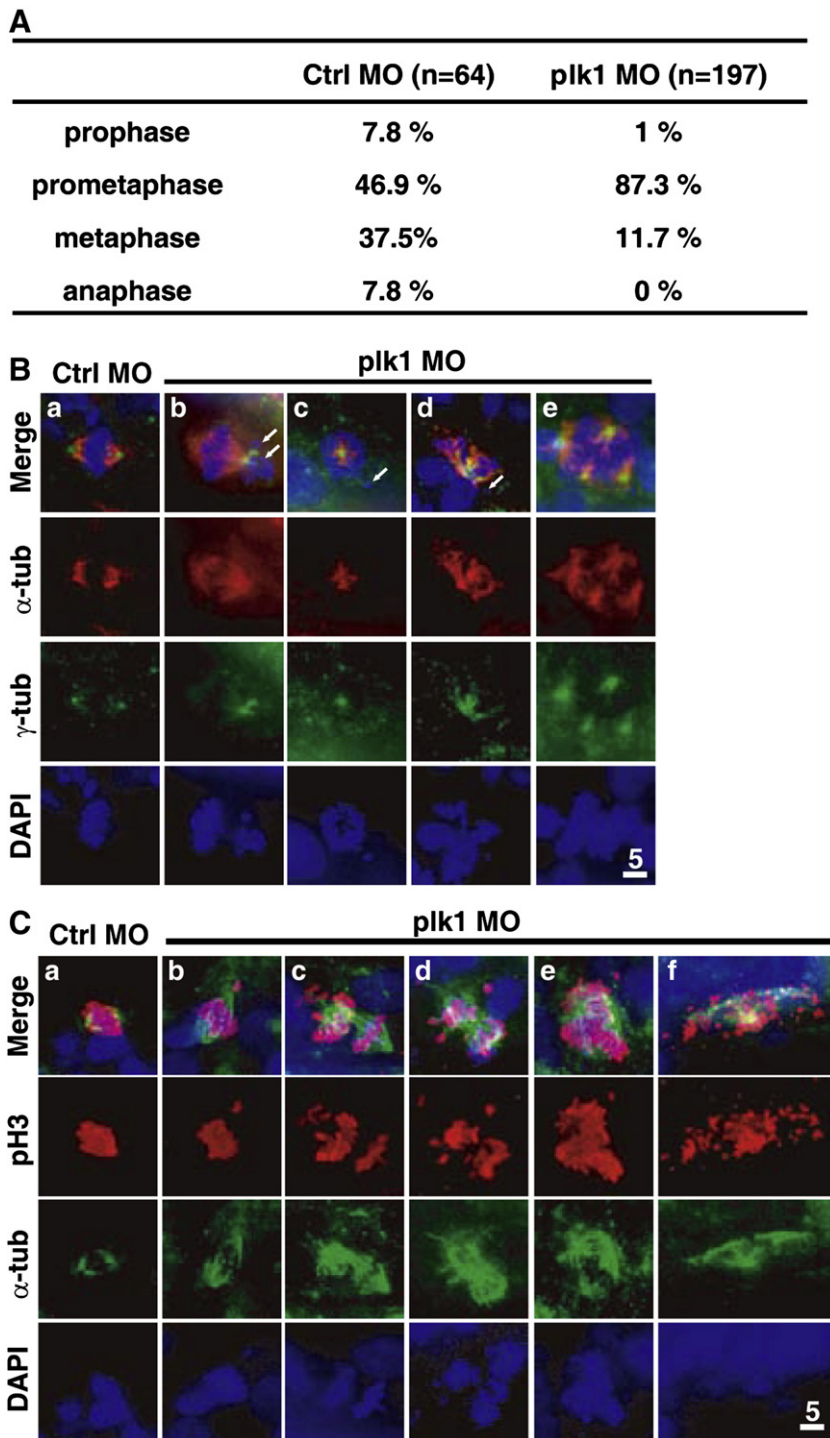


Fig. 3. Plk1 depletion leads to prometaphase arrest in zebrafish embryos, accompanied by congression failure and mitotic spindle abnormality. (A) A comparison of the percentage of cells in the indicated stages of mitosis, as judged by the degree of chromosome condensation, nuclear envelope breakdown (NEBD), and chromosome arrangement relative to spindle microtubules. (B) Embryos injected with 0.5 pmol of control or *plk1* ATG MO were co-immunostained with anti- α -tubulin and anti- γ -tubulin antibodies at 24 hpf. Red, α -tubulin; green, γ -tubulin. Arrows mark uncongressed chromosomes. (C) Analyses of single cells from the embryos of Fig. 2H (and supplemental Fig. 2). Scale bar, 5 μ m.

chromosomes and activation of SAC (Acquaviva et al., 2004). Therefore, it is likely that all of the observed mitotic infidelity induced the activation of SAC and subsequent growth arrest in *plk1* morphants.

Plk1 knockdown results in chromosome instability in zebrafish embryos

To analyze the chromosome number, single cell suspensions were prepared from morphant embryos at 28 hpf, and their DNA contents

were analyzed (Fig. 4A). Cells isolated from the control morphants displayed the typical high 2 N DNA and lower 4 N DNA peaks that are found in proliferating cells (Fig. 4A, straight blue line). In comparison, cells of the *plk1* morphants displayed markedly lower 2 N and higher 4 N DNA contents, and a broad range of cells exhibited \sim 8 N DNA contents, indicating the presence of polyploid cells, including the cells arrested in M phase. The sub-G1 population of cells, which is indicative of apoptotic cells, was markedly increased in *plk1* morphants (Fig. 4A, broken line).

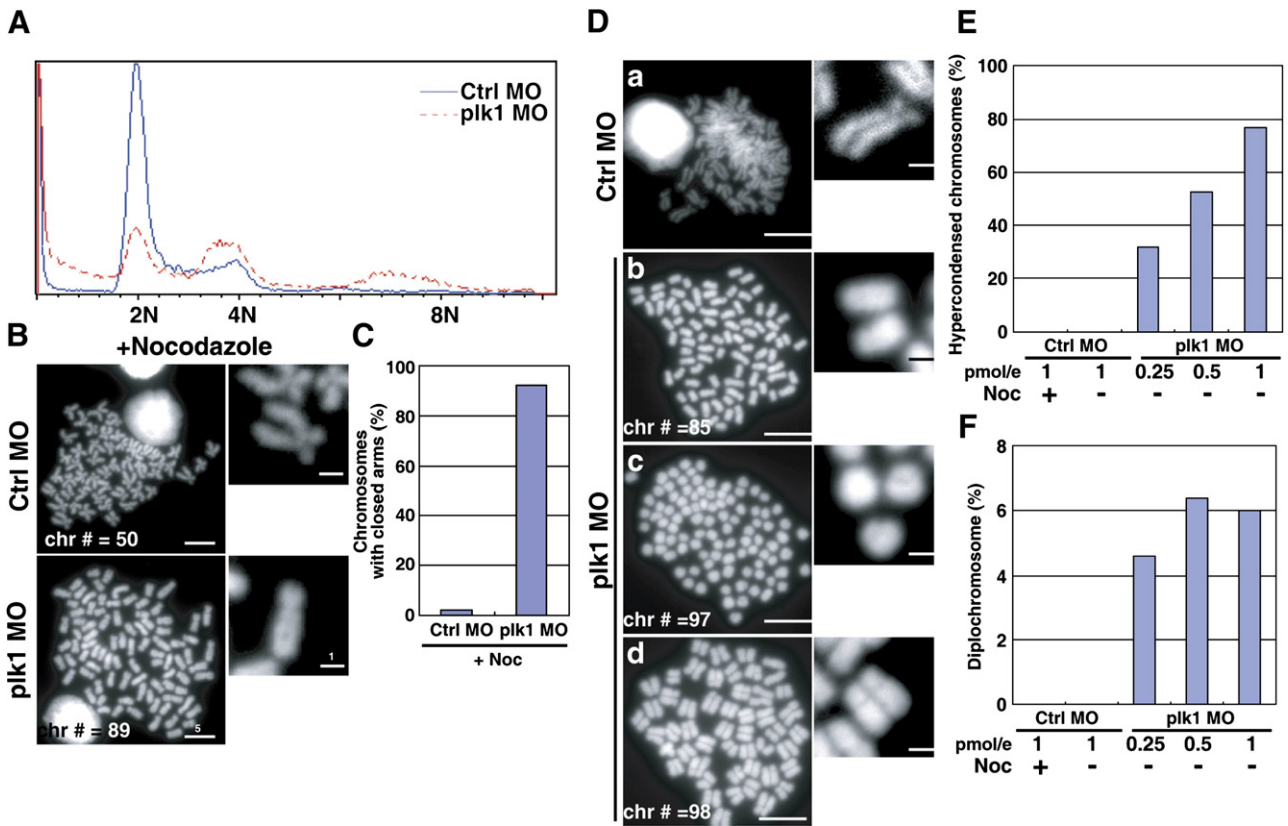


Fig. 4. Severe chromosome abnormalities in *plk1* morphant embryos. (A) Embryos were injected with 0.25 pmol of control or *plk1* ATG MO and single cell suspensions were prepared at 28 hpf. DNA contents were measured by Propidium iodide (PI) staining and flow cytometry. (B) Metaphase chromosome spreads from control (Ctrl MO) or *Plk1* morphants (Plk1 MO). Chromosome numbers (Chr #) and scale bars are indicated. Enlarged images are shown at the right. (C) Chromosomes with closed arms were counted in control or *plk1* morphants and compared and represented as percentages in a bar graph. (D) Representative chromosome spreads prepared without nocodazole treatment. Scale bar, 5 μ m. (E) The ratio of hypercondensed chromosomes (Dc), scored from 150 metaphase spreads of 20 embryos each. Data from control morphants treated with nocodazole were included for control. (F) The presence of diplochromosomes (Dd) in *plk1* morphants.

Next, embryos from control and *plk1* morphants were subjected to metaphase chromosome spreads to characterize chromosomal abnormalities. Diploid zebrafish cells have 50 chromosomes (Fig. 4B, Ctrl MO). In comparison, the chromosome number in *plk1* morphants was heterogeneous from cell to cell, indicative of aneuploidy (Fig. 4B, Plk1 MO). These data confirmed that Plk1 depletion results in chromosome number aberrations in zebrafish embryos.

One of the significant features of the metaphase chromosomes prepared from *plk1* morphants was a high incidence of closed chromosome arms (92%, $n=38$), while chromosome spreads from control morphants displayed open chromosome arms (98%, $n=50$) (Fig. 4B–C). Polo-like kinase phosphorylates cohesins in prophase, which leads to the dissociation of cohesins from chromosome arms in prophase and prometaphase (Hauf et al., 2005; Losada et al., 2002; Sumara et al., 2002). Prolonged nocodazole treatment leads to hyperactivation of Plk1, leading to dissociation of cohesins from chromosome arms, but not of centromeric cohesion until anaphase, resulting in open arm (X-shaped) chromosomes in human metaphase cells (Gimenez-Abian et al., 2004). It is thought that the resolution of cohesion in *Drosophila* and mammals occurs in two steps: first, the dissociation of cohesion from chromosome arms in prophase-prometaphase, followed by the cleavage of centromeric cohesion by separase in anaphase onset (Nasmyth, 2002; Nasmyth and Haering, 2009; Watanabe and Kitajima, 2005). Meanwhile, the prophase-prometaphase contribution of chromosome arm separation in yeast is not significant; thus, the chromosome separation occurs in one step (Lee et al., 2005; Nasmyth and Haering, 2009; Peters et al., 2008). Analysis of metaphase chromosomes in *plk1* morphant embryos (Fig. 4B–C) suggested that chromosome separation in zebrafish is likely to occur in two steps, as it does in mammals, and that Plk1 is required for

the dissociation of cohesins from chromosome arms in prophase-prometaphase.

Next, we analyzed the mitotic chromosomes in the absence of nocodazole. In control morphant cells, condensed chromosome spreads were rarely found (Fig. 4Da). In comparison, the chromosomes of *plk1* morphants were highly condensed even without nocodazole treatment, consistent with our notion that Plk1 depletion induces prometaphase arrest (Fig. 4Db–d and E). Interestingly, hypercondensed chromosomes, which are characterized by extremely short chromosome arms with indistinguishable centromeres were observed in *plk1* morphants (Fig. 4Dc). The frequency of chromosome spreads exhibiting these short hypercondensed chromosomes increased as the concentration of *plk1* morpholino increased (Fig. 4E). These results suggest that Plk1 regulates chromosome condensation.

A small number of chromosome spreads from *plk1* morphants exhibited diplochromosomes, which are composed of two pairs of sister chromatids linked together. These diplochromosomes are thought to result from a failure of sister chromatid arm separation that continued during the replication of chromosomes in the subsequent cell cycle (Ghosh et al., 1993) (Fig. 4Dd and F). Diplochromosomes have been observed in separate mutants in *Drosophila*, mouse, and zebrafish (Goyanes and Schwartzman, 1981; Kumada et al., 2006; Shepard et al., 2007; Stratmann and Lehner, 1996). We interpreted these observations, as follows: *Plk1* knock-down during zebrafish embryogenesis results in the failed dissociation of cohesion along the arms and centromere, premature mitotic exit, and chromosome duplication in the subsequent cell cycle. Embryos treated with nocodazole did not show any diplochromosomes ($n=382$) because nocodazole treatment prevented these cells from exiting mitosis in *plk1* morphants. Collectively, these data

suggest that Plk1 is also involved in mitotic exit. However, in zebrafish embryogenesis, Plk1 is primarily required for mitotic progression rather than mitotic exit, as illustrated by a low percentage (1–8%) of diplochromosomes. We speculate that this is because mitosis precedes mitotic exit and indicates that in rapid and continued cell division of zebrafish embryogenesis, Plk1 is primarily needed in mitosis.

Live-imaging reveals that Plk1 is essential, whereas Plk2 and Plk3 are dispensable in mitosis of living embryos

We considered that visualization of cell division after *Plk1* depletion in living organisms might be the most persuasive way to establish the functions of Plk1 in development. Towards this end, zebrafish has many advantages because their embryos are transparent and their development is rapid. Taking these advantages into account, we attempted to observe and record cell division events before and after morpholino injection of live embryos.

We first made a transgenic zebrafish that expresses a GFP-tagged histone, H2B-GFP. Twenty hours after injection of morpholino oligos into the embryos of these transgenic fish, chromosome movements and cell division were recorded at the single cell level using time-lapse microscopy.

Cells from the control morphants underwent mitosis for an average of 16.9 ± 3.3 min ($n = 48$ from 14 embryos) from the point of nuclear envelope breakdown (NEBD) to chromosome segregation to opposite poles (Fig. 5A and I, supplemental Movie 1). In comparison, *plk1* morphant cells remained in mitosis for 190.1 ± 127.1 min (Fig. 5B–E and I). As shown in Table 1, the arrest was not permanent: 57.1% of *plk1* morphant cells were delayed in mitosis but finally segregated their chromosomes; 28.6% segregated with uncongressed chromosomes (white arrow in Fig. 5B, Supplementary movie 2); and 14.3% displayed Polo-type chromosomes and were delayed in mitosis. These cells exited mitosis without segregation (Fig. 5C, supplementary Movie 3). Chromatin bridges (Fig. 5D, white arrow, supplemental Movie 4) and multiple metaphase plates were frequently observed, and a single cell often gave birth to three or more aneuploid cells (Fig. 5E, supplemental Movie 5). The death of mitotic cells was not observed during the course of the recording, suggesting that apoptosis (Fig. 2) occurs later (Table 1).

Plk2 and Plk3 resemble Plk1 in structure, and the small molecule inhibitor BI 2536, which specifically blocks Plk1 activity, can also block the kinase activities of Plk2 and Plk3 *in vitro* when used in higher concentrations than what is needed to specifically inhibit Plk1 (Steegmaier et al., 2007). To examine if remaining Plk2 or Plk3 compensated for the depletion of Plk1, we monitored the effects of knockdown gene expression of *Plk2* and/or *Plk3*. Time-lapse microscopy of *Plk2* and/or *Plk3* morphant embryos revealed that *Plk2* and *Plk3* were dispensable for progression into mitosis in zebrafish embryos: the mitotic timing of *plk2* morphants (Fig. 5F and I, supplemental Movie 6) or *plk3* morphants (Fig. 5G and I, supplemental Movie 7) were similar to controls (Fig. 5A and I). In addition, embryos depleted of *Plk2* or *Plk3* did not display any significant abnormalities (data not shown). Mitotic infidelities observed in *plk1* morphant embryos were not observed in *plk2* or *plk3* morphants (Fig. 5F–H). Co-injection of *Plk2* MO and *Plk3* MO also

did not cause any abnormalities in mitosis (Fig. 2H and I). These results suggest that *Plk1* is essential, while *Plk2* and *Plk3* are dispensable for mitosis in zebrafish. Live-imaging of whole embryos

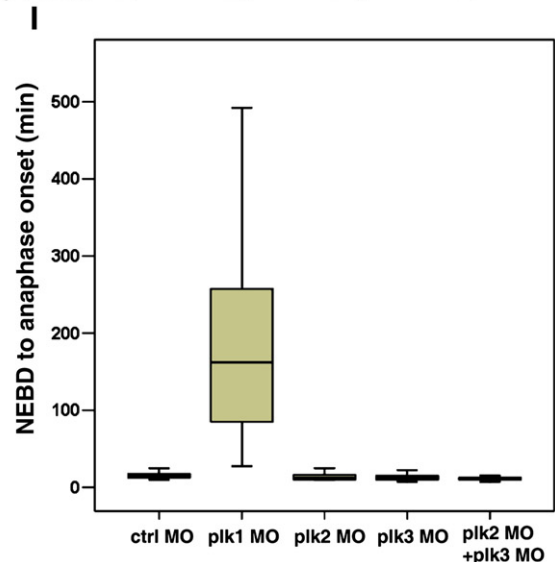
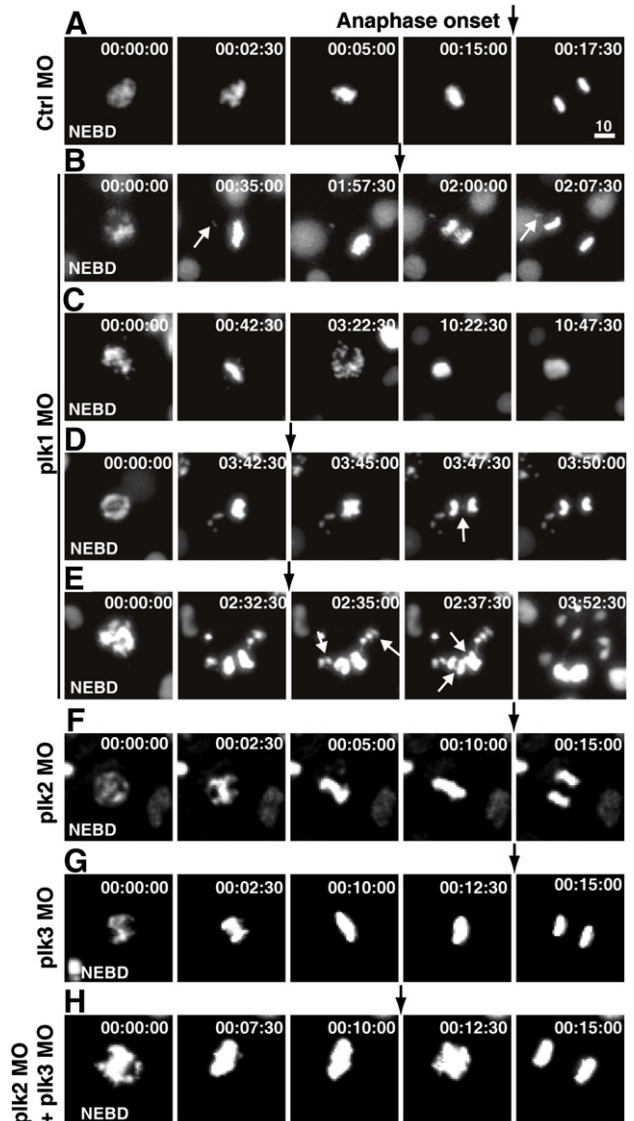


Fig. 5. Live-cell imaging reveals that Plk1 is essential in mitotic progression, but Plk2 and Plk3 are dispensable in zebrafish embryos. (A–H) Transgenic zebrafish embryos expressing H2B-GFP were injected with 0.5 pmol of control (A), *plk1* ATG MO (B–E), *plk2* splicing MO (F), *plk3* splicing MO (G), *plk2* splicing MO and *plk3* splicing MO (H, supplemental movie 8). The surface of the yolk was subjected to time-lapse microscopy, and images were captured every 2.5 min in 22 hpf embryos. The time from NEBD is shown as h:min:s. Black arrows mark the point of anaphase onset. White arrows mark the uncongressed chromosomes in B, lagging chromosomes in D, and multiple metaphase plates in E, respectively. Scale bar, 10 μ m. (I) Box plots of mitotic timing, measured from NEBD to the onset of anaphase. At least 30 cells from more than five embryos each were scored. Bars within the boxes are the median values, as determined by statistical analysis using SPSS software.

Table 1
Analysis of mitosis in Plk1-depleted zebrafish embryos.

	Ratio (%)	
	control MO	<i>plk1</i> MO
Normal segregation	100	0
Segregation after mitotic delay	0	57.1
Segregation with uncongressed chromosomes	0	28.6
Mitotic slippage	0	14.3
Number of embryos examined	<i>n</i> = 5	<i>n</i> = 8
Total cell number	<i>n</i> = 116	<i>n</i> = 154

supported our previous interpretation that mitotic infidelities by the depletion of Plk1 induced SAC activation and subsequent mitotic delay (Fig. 5I).

Next, we made more precise characterizations of the aberrant chromosome segregation (Gisselsson, 2008) and asked whether the chromosome abnormalities became more severe with time. Defects observed in Plk1-depleted cells before 24 hpf displayed multipolar segregation (14.3%), lagging chromosomes (14.2%), or chromatin bridges (7.9%). Six percent of cells exited mitosis without chromosome segregation. Mitotic infidelity became more severe with time in development; the number of cells that managed to correct the problem and enter anaphase was decreased at 26 hpf compared to 24 hpf (Table 2).

BI 2536, a Plk1 inhibitor developed in cancer cell lines, blocks mitotic progression in developing zebrafish embryos

Cancer cells exhibit an unlimited proliferative capacity; hence, regulating the proliferation of cancer cells has been one of the major approaches of cancer therapy. The development of inhibitors for mitotic kinases has attracted considerable attention, and a number of them are currently being tested in clinical trials (Taylor and Peters, 2008). BI 2536 was developed through efforts to screen for small molecules that specifically inhibit Plk1 (Lenart et al., 2007; Steegmaier et al., 2007). As we observed that Plk1 was required for embryonic proliferation and, thus, was needed for zebrafish embryogenesis, we asked whether BI 2536 could inhibit Plk1 function in zebrafish embryos. We also considered that zebrafish embryogenesis could be a useful *in vivo* system for validating the effects of mitotic kinase inhibitors, such as anti-cancer drugs.

Soaking the dechorinated early stage embryos in BI 2536-treated egg water resulted in massive embryonic death, even at low concentrations (100 nM). Therefore, we optimized the timing and dose of the BI 2536 treatment to analyze the effect of Plk1 inhibition at the cellular level. As a result, we found that 100 μ M of BI 2536 treatment to 22 hpf embryos was best for observing the effects of the drug on cell division.

Table 2
Mitotic timing from NEBD to the onset of anaphase in *plk1* morphants.

	Before 26 hpf		After 26 hpf	
	(%)	Duration (min) (mean \pm sd)	(%)	Duration (min) (mean \pm sd)
Segregation after delay	55.6	86.6 \pm 60	33	149 \pm 78.1
Multipolar segregation	14.3	116.7 \pm 49.8	12.1	188.4 \pm 88.3
Lagging chromosomes	14.2	136.9 \pm 68.3	4.4	255 \pm 107.4
Chromatin bridges	7.9	181.5 \pm 74.1	23	252.3 \pm 92.9
Multiple defects	1.6	170 \pm 0	7.7	236.1 \pm 63.2
Mitotic slippage	6.4	313.1 \pm 94.8	19.8	396.1 \pm 137.5
Total cell number	63		91	

H2B-GFP transgenic embryos, which were generated to facilitate the monitoring of chromosome movements, were injected with morpholino oligos for control, *plk1*, *plk2*, *plk3*, or *plk2* MO + *plk3* MO. Then the embryos were let to develop for 24 hours. The drug was applied at 24 hpf and incubated for 2 h at room temperature. Then the embryos were subjected to time-lapse microscopy for more than 16 h with continuous treatment of 100 μ M BI 2536 (Fig. 6A).

Compared to the one- to four-cell stage embryos, BI 2536 toxicity was markedly reduced in 22 hpf embryos. However, the live-imaging explicitly showed that the mitotic timing was markedly delayed in the cells of the BI 2536-treated embryos: timing from NEBD to anaphase onset took \sim 14 min in the control (Fig. 6B, Supplemental movie 9), whereas cells of the BI 2536-treated embryos were arrested in mitosis for at least \sim 10 h (Fig. 6C, supplemental Movie 10). Similar to the *plk1* morphants, uncongressed chromosomes were apparent in the control morphant cells treated with BI 2536 (Fig. 6C). Notably, BI 2536-treated embryos exhibited more severe phenotype compared to *plk1* morphants. Plk1-depleted cells were delayed in mitosis for \sim 200 min, but \sim 86% of those eventually segregated (Table 1). By comparison, cells from BI 2536-treated embryos never segregated their chromosomes during the 16 h recording. Some *plk1* morphant cells exited from mitosis without dividing (Fig. 6C–G and H). Another prominent feature of the BI 2536-treated embryos was the dominance of monopolar spindles, whereas *plk1* morphants displayed multipolar spindles (51%) and much less monopolar spindles (5.5%).

The concentration of BI 2536 that was required in zebrafish embryos was 1,000-fold higher than the minimum amount required to inhibit Plk1 in cultured cells. At such high concentrations, BI 2536 can also inhibit the kinase activities of Plk2 and Plk3 (Steegmaier et al., 2007). Therefore, we tested whether Plk2 or Plk3 kinase activities were inhibited in 100 μ M of BI 2536, *in vitro*. Indeed, *in vitro* kinase assays revealed that the addition of 100 μ M of BI 2536 completely blocked all three kinase activities (supplemental Fig. S4). However, Plk2 and Plk3 were dispensable in embryonic proliferation (Fig. 5). Therefore, it is likely that the effect of BI 2536 treatment resulted from inhibiting Plk1, and not Plk2 or Plk3 *in vivo*. Nevertheless, we asked whether the mitotic arrest and defective cell division caused by 100 μ M BI 2536 *in vivo* were due to the inhibition of Plk2 and Plk3, as well as Plk1.

BI 2536 was added to embryos injected with *plk1* MO-, *plk2* MO-, *plk3* MO, or *plk2* MO + *plk3* MO. Because BI 2536-treated embryos never segregated during the experiment, but some chromosomes decondensed without segregation, we measured the timing from NEBD to mitotic exit. Intriguingly, *plk1* morphants treated with BI 2536 exhibited the most severe phenotype in that the NEBD to mitotic exit timing was the longest (\sim 14 h, Fig. 6H). By comparison, mitotic infidelities by the BI 2536 treatment to embryos injected with *plk2* MO, *plk3* MO, or the combination of both, all resembled the control cells treated with the drug (Fig. 6E–G). The timing from NEBD to mitotic exit was similar as well (Fig. 6H). This result is consistent with the observation that *plk2*- and *plk3* morphant embryos did not display any mitotic abnormalities (Fig. 5F–I). Taken together, the mitotic arrest and the absence of cell division in BI 2536-treated zebrafish embryos is likely to result from complete inhibition of Plk1, *in vivo*. It is thought that the reason why BI 2536-treated embryos exhibited a more severe phenotype compared to *plk1* morphants is because BI 2536 treatment is more effective compared to knockdown expression of *Plk1* by morpholino injection. Combination of both *plk1* MO injection and BI treatment resulted in maximal phenotype (Fig. 6D) supports this interpretation.

To confirm the “Polo-type” spindle formation in the BI 2536-treated embryos, BI 2536-treated or untreated embryos were subjected to immunostaining with α -tubulin and γ -tubulin antibodies. Indeed, the BI 2536-treated embryos exhibited monopolar spindles (Fig. 6F), as was observed in HeLa cells (Lenart et al., 2007). In the developing embryos, the drug effectively blocked the cells from

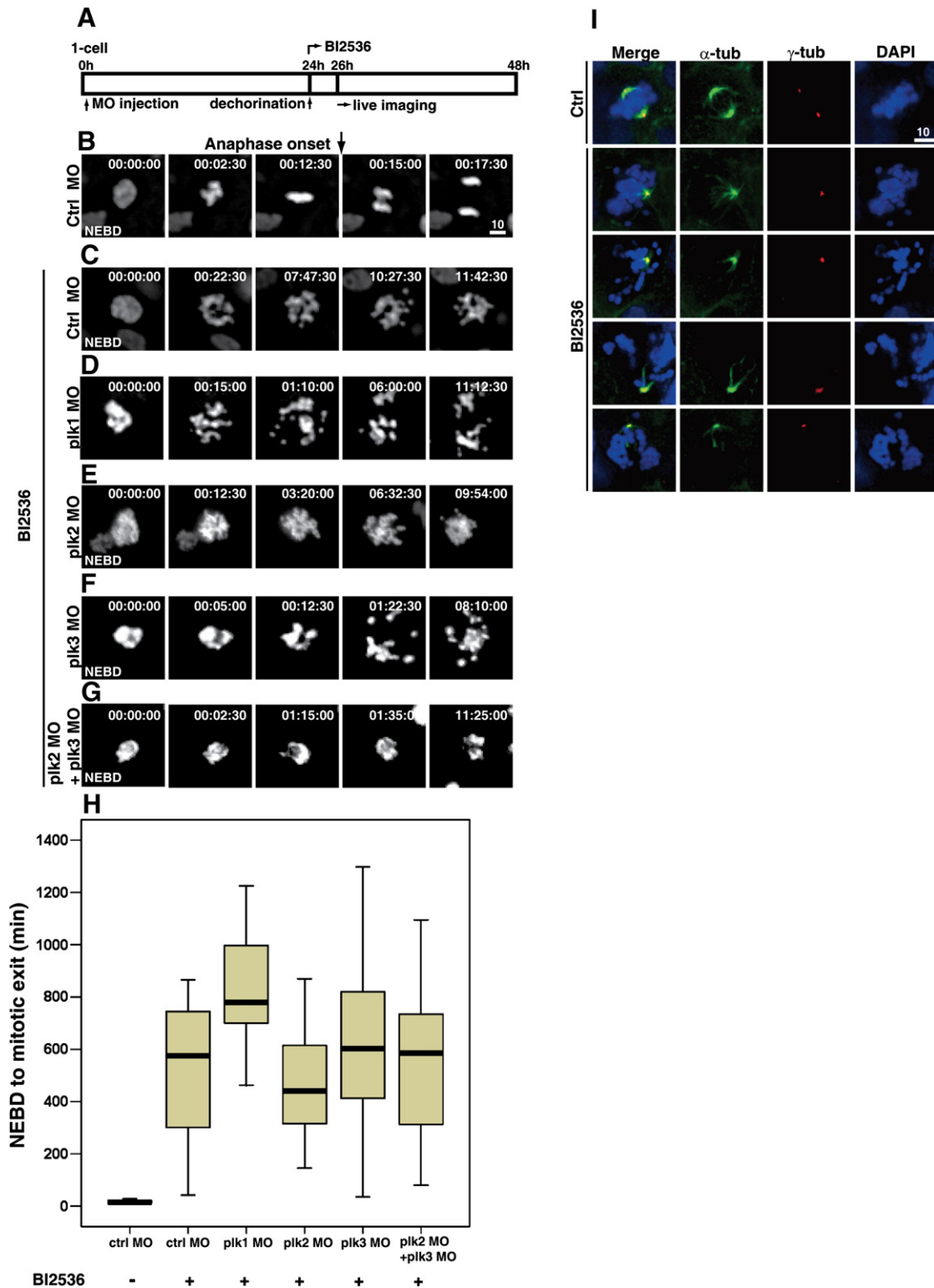


Fig. 6. Treatment of 24 hpf embryos with BI 2536, the small molecule inhibitor specific for Plk1, leads to mitotic infidelity and prometaphase arrest. (A) Scheme of BI 2536 treatment in developing zebrafish embryos. Embryos at one- to four-cell stage were injected with indicated morpholino oligos and the drug was treated at 24 hpf. (B) Captured images of cells from the control embryos. The black arrow marks the timing of anaphase onset. The time at NEBD was set to 0. (C–G) Captured images of BI 2536-treated embryos after the injection of indicated morpholinos (supplemental movies 10–14). (H) Box plots of timing from NEBD to mitotic exit. More than 50 cells from at least five embryos each were analyzed. Bars within the boxes are the median values, determined by statistical analysis using SPSS software. Note that BI 2536 treatment in *plk1* morphants exhibit more severe phenotype compared to others. (I) Immunofluorescence of the fixed embryos with anti- α -tubulin and γ -tubulin with or without BI 2536 treatment. Note the monopolar spindles in BI 2536-treated embryos.

entering anaphase. We were not able to control cytokinesis with this drug, as in HeLa cells (Lenart et al., 2007). Taken together, BI 2536 inhibited Plk1 function and arrested cells in mitosis during zebrafish development. These results establish zebrafish embryogenesis as an

efficient model system to validate the effects of mitotic kinase inhibitors. The live-imaging technique of developing zebrafish embryos used here could be applied to screens for effective inhibitors for Plk and other mitotic kinases. Furthermore, the zebrafish system

may prove to be a promising *in vivo* validation system for anti-cancer drugs.

Imbalanced Plk1 activity leads to mitotic infidelity

In this study, we have developed compelling lines of evidence that inhibition or knockdown of *Plk1* expression interferes with mitotic progression and can trigger chromosome instability. In numerous reports, elevated expression of *Plk1* has been observed in many cancers (Smith et al., 1997; Takai et al., 2005). Therefore, we asked whether over-expression of *Plk1* affects embryogenesis. We injected RNAs encoding *GFP*; wild-type *Plk1*; the kinase dead mutant *K68R*, where the ATP-binding pocket of the kinase domain is mutated; the non-degradable D-box mutant *R324A* (Lindon and Pines, 2004); and the PBD domain mutant *W414F* (Lee et al., 1998) (Fig. 1A). All *Plk1* constructs were fused to GFP at their N-terminus to detect ectopic *Plk1* expression.

GFP-plk1 or *GFP* sense RNAs were injected into the yolk of one-cell stage embryos and the expression of GFP was monitored by fluorescence microscopy. The levels of GFP expression between embryos injected with *GFP* alone or various RNAs of *GFP-Plk1* were indistinguishable until the end of gastrulation, after which the GFP fluorescence of the *wild-type*, *K68R*, and *W405F* expressing embryos rapidly decreased. The fluorescence intensity of the D-box mutant *R324A* decreased to a much lesser extent (data not shown).

Next, we investigated any change in mitotic cells after RNA injection. Embryos were fixed at the 18-somite stage and stained with anti-pH3 antibody. The number of pH3-positive cells increased markedly in embryos injected with the wild-type, *K68R*, *W405F*, and

to a moderate level in *R324A* compared to the control *GFP*-injected embryos (Fig. 7A). Interestingly, a significant number of cells in embryos of the wild-type (100%, $n = 13$), the kinase-dead mutant *K68R* (100%, $n = 12$), the D-box mutant *R324A* (61.5%, $n = 13$), and the PBD-box mutant *W405F* (80%, $n = 10$) displayed highly disorganized mitotic chromosome arrangements, as revealed by immunostaining with anti-pH3 (Fig. 7A, inner box), which is indicative of mitotic infidelity in these embryos. These results suggest that over-expression of either the wild-type or the mutants resulted in a defective chromosome arrangement in mitosis. This observation is in accordance with the reports from HeLa cells, which showed that the over-expression of wild-type or kinase-dead *Plk1* resulted in mitotic arrest (Mundt et al., 1997; Tang et al., 2006). Taken together, both over-expression and inhibition of *Plk1* result in problem in mitosis; therefore, a balanced level and function of *Plk1* is required for proper mitotic progression.

Finally, we determined which domain of *Plk1*, the kinase domain, D-box, or PBD domain, was most responsible for its function during mitosis. We injected various *Plk1* RNAs simultaneously with the *plk1* MO at the one-cell stage and analyzed the ability of each mutant to rescue the *Plk1* depletion phenotype. The embryos were fixed at the 18-somite stage, and the pH3-positive mitotic cells were identified. Because *plk1* ATG MO was designed to block the translation of endogenous *plk1* specifically, it did not interfere with the translation of *GFP-Plk1*. To avoid the effect of *Plk1* over-expression (Fig. 7A), we were careful to optimize the amount of RNA injected.

Injection of wild-type and *R324A* partially rescued the disorganized chromosomes (Fig. 7B, inner box) and mitotic arrest

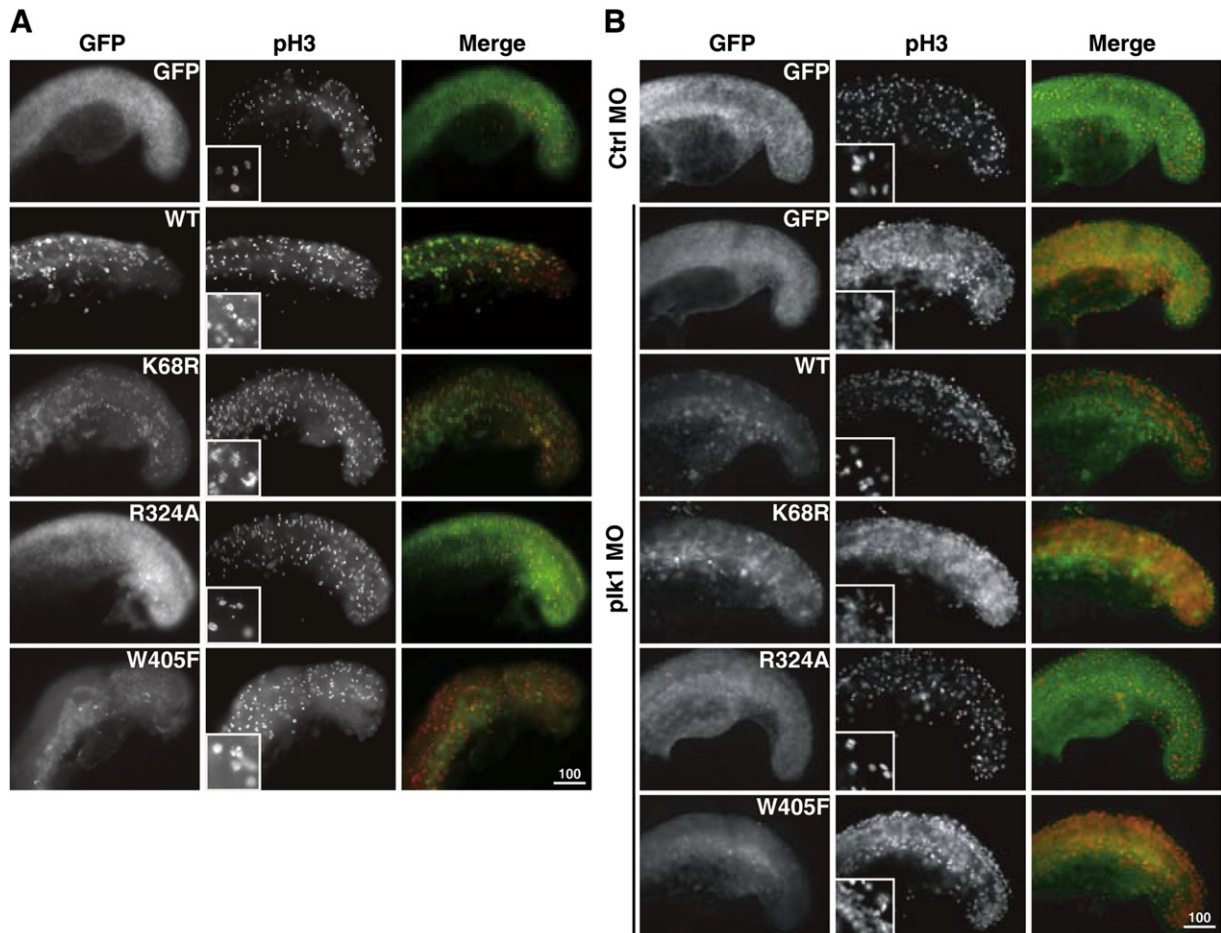


Fig. 7. Injection of wild-type *Plk1*, kinase-dead mutant, D-box mutant, and PBD domain mutant RNAs (illustrated and marked in Fig. 1A) in wild-type and *plk1* morphant embryos. Embryos were injected with various *GFP-plk1* RNAs alone (A) or in combination with *plk1* MO (B). Embryos were collected at the 18-somite stage and stained with anti-pH3 antibodies (red) to assess the effect of the expression of these RNAs on mitosis. Enlarged images of chromosomes stained with anti-pH3 are shown in the inner box for comparison.

phenotypes (Fig. 7B, number of pH3-positive cells, red) caused by *plk1* MO: the percentage of embryos with disorganized chromosomes immunostained with anti-pH3 antibodies was 100% ($n = 22$) for GFP-injected embryos; 31.25% for wild-type *Plk1*-injected embryos ($n = 16$); and 33.3% in *R324A*-injected embryos. In contrast, injection of *K68R* or *W405F* RNA was not capable of rescuing the mitotic defects: 95% ($n = 20$) of *K68R*-injected embryos and 100% ($n = 12$) of *W405F*-injected embryos displayed disorganized chromosomes. The number of pH3-positive cells in embryos injected with *K68R* or *W405F* with *Plk1* MOs was increased even more compared to control *plk1* morphant embryos (GFP alone); this treatment exacerbated the mitotic defects (Fig. 7B, inner box). These results indicate that both the kinase and the PBD domains are required during mitosis, *in vivo*, consistent with previous reports from structural studies and cell culture systems. The substrate-specific kinase activity of Plk1 is coordinated by the kinase and PBD domains (Cheng et al., 2003; Elia et al., 2003a,b; Garcia-Alvarez et al., 2007; Kang et al., 2006; van de Weerd et al., 2008). The reason why the D-box mutant *R324A* was able to rescue the mitotic defect of the *plk1* morphants may be because Plk1 is degraded after mitosis, during mitotic exit (Lindon and Pines, 2004); thus, during mitosis, *R324A* would behave like the wild-type.

Discussion

Mitosis and development

Cell cycle regulators play crucial roles during development (Budirahardja and Gonczy, 2009). The asymmetric distribution of Plk1 in *Caenorhabditis elegans* differentially regulates the duration of the cell cycle in two-cell stage embryos and contributes to fate determination by establishing cell polarity (Budirahardja and Gonczy, 2008; Rivers et al., 2008). This finding suggests that the timing of mitosis, duration of mitotic entry, and mitotic progression are all coupled to cell fate determination during development.

We have shown here that zebrafish embryogenesis requires Plk1 for mitotic progression and proliferation. We were not able to assess the role of *Plk1* in early embryogenesis because Plk1 was expressed maternally and the morpholino was not effective before gastrulation. Nevertheless, we have shown that *Plk1* is essential for mitotic chromosome homeostasis and bipolar spindle assembly after gastrulation, implying that it may play similar roles in early embryos.

Plk1 knockdown resulted in deregulated chromosome condensation, impaired cohesin dissociation/chromosome arm separation, irregular spindle organization, and multipolar or monopolar centrosomes. These features are reminiscent of the chromosome instability observed in cancer cells; thus, the results presented here have implications in the understanding of chromosome instability in cancer.

In the metaphase chromosome spreads, we found that Plk1 is required for proper chromosome condensation and chromosome arm separation in embryogenesis. In addition, through attempts to rescue the *plk1* morphant phenotype, we found that the kinase activity of Plk1 was required for its mitotic functions. These results raise an important question regarding the downstream targets of Plk1 in chromosome homeostasis that should be addressed in the future. When zebrafish genetics, morpholino technology, and the cell biology assays shown in this work are combined, the discovery of the critical substrates of Plk1 in chromosome condensation and cohesion may be achieved.

Injection of wild-type, kinase-dead mutant, non-degradable mutant, and PBD domain mutant RNAs all resulted in disorganized chromosomes when endogenous *Plk1* was present. Taken together with the results of the rescue experiment (Fig. 7B), these findings suggest that maintenance of the level of intact Plk1 *per se* is critical for mitotic fidelity and development.

Plk1 depletion and the activation of SAC

We showed here that Plk1 depletion results in mitotic delay and embryonic growth defects. Cells from *plk1* morphant embryos were arrested in mitosis, as evidenced by the time course experiment of double BrdU/pH3 staining and live-imaging. These were accompanied by a marked increase of MPM-2 staining and prometaphase cells. To assess the activation of SAC, we asked for the localization of BubR1 and Mad1/Mad2 at the kinetochores. However, because the antibodies against the core SAC components did not work in zebrafish, we were not able to confirm the activation of SAC by immunofluorescence. Therefore, we cloned zebrafish *Mad1*, linked it to GFP, and utilized the GFP-Mad1 fluorescence to assess the activation of SAC. Previously, it was suggested that phosphorylation of Mad1 by Plk1 is required for kinetochore localization of Mad1/Mad2 and the consequent activation of SAC (Chi et al., 2008). However, in zebrafish, Plk1 depletion did not interfere with Mad1 localization at the kinetochores. Notably, the number of prometaphase cells, with Mad1 at the kinetochores, increased markedly in zebrafish embryos injected with *plk1* MO even compared to nocodazole-treated embryos. These results suggest that SAC is activated upon depletion of Plk1 in zebrafish embryos. This interpretation is in agreement with a report from HeLa cells: BI 2536-treated HeLa cells display mitotic delay and increased Mad2 localization at the kinetochores, indicative of SAC activation (Lenart et al., 2007). Mad1 is required for Mad2 to localize to the kinetochores. Therefore, we assume that Mad2 localization at the kinetochores is likely to have been increased, along with Mad1, in *plk1* morphants. Thus, the results presented here demonstrate that Plk1-mediated phosphorylation may not be crucial for Mad1 localization, and the activation of SAC, in zebrafish. The discrepancy between zebrafish and cultured cells (Chi et al., 2008) is not understood.

Visualizing mitosis in developing embryos

Mitosis is a carefully orchestrated sequence of events. Each mitotic event is dependent on previous events in a spatiotemporal- and stage-dependent manner. Thus, the visualization of this orchestration is essential for understanding the fundamentals of mitosis. A single cell live-imaging technique has been developed for cultured mammalian cells, which has resolved many controversial details of mitotic mechanisms (Hagting et al., 2002; Kanda et al., 1998; Lindon and Pines, 2004; Nilsson et al., 2008).

In this study, we adopted this single cell live-imaging technique for use with whole zebrafish embryos. Live-imaging of a living organism, combined with the rapid development and *ex vivo* embryogenesis of zebrafish, enabled us to functionally validate the effects of BI 2536 in live embryos. This Plk1 inhibitor was originally developed through chemical library screens conducted in cultured cancer cell lines, in which a number of critical mutations in variable checkpoint responses, apoptosis, and DNA repair exist. Therefore, the efficacy of the drug can differ from cell line to cell line and in cancer patients. With live-imaging in whole embryos, we were able to observe that BI 2536 specifically interfered with mitotic events, such as bipolar centrosome formation/maturation and chromosome congression in proliferating zebrafish embryos. Interestingly, BI 2536 treatment resulted specifically in the formation of monopolar spindles, while *plk1* MO injection produced multipolar, and a few monopolar, centrosomes. This difference suggests that centrosome formation, separation, and maturation are all coordinated, but individual events are mediated by the degree of Plk1 activity. Taken together, our results validate the effects of Plk1 inhibition by BI 2536 in zebrafish development. Furthermore, these results imply that the potential of using zebrafish embryogenesis for screening and validation of anti-mitotic drugs is promising with respect to cost and time.

Plk1 is essential, but Plk2 and Plk3 are dispensable, in zebrafish embryogenesis

Despite the severe phenotypes of *Plk1* depletion at the cellular level, massive cell death was not observed in *plk1* morphants until 6 dpf. This lower sensitivity of zebrafish embryos to *Plk1* knockdown may be due to the presence of maternal *Plk1* proteins. However, other Polo-like kinases, *Plk2*, *Plk3*, and *Plk4* are present in zebrafish, as they are in human cells: therefore, the possibility remained that the other Plk proteins compensated for the loss of *Plk1* in mid-to-late zebrafish embryos. To assess this possibility, we examined the phenotypes of *Plk2* and *Plk3* depletion by morpholino injection. The result showed that *Plk2* and *Plk3* are largely dispensable in embryogenesis. Although the functions of *Plk2* and *Plk3* are not fully established, reports suggest that they have functions in the interphase checkpoint or replication (Archambault and Glover, 2009). Since we have extensively examined their effects in mitosis, but not in interphase, the possibility that *Plk2* or *Plk3* has some roles in interphase upon environmental attacks still remains. Nevertheless, we have shown that *Plk1* is crucial, while *Plk2* and *Plk3* are dispensable, in mitotic fidelity and embryogenesis. Because *Plk4* is more structurally different than the other Plks and has specific functions, we did not investigate the outcome of the loss of *Plk4* in this study and left it for future studies. However, haploinsufficiency of *Plk4* in mice results in mitotic infidelity and carcinogenesis due to multipolar centrosomes and spindle irregularities (Ko et al., 2005), similar to our observations of *Plk1* depletion in zebrafish. Therefore, the possibility that *Plk4* partially compensates for the loss of *Plk1* during zebrafish development is not fully excluded.

Acknowledgments

The Tol2 transposable element system used for generating the zfh2B-GFP zebrafish was a generous gift from Dr. Kawakami of the National Institute of Genetics, Japan. This work was supported by the Basic Science Research Program through the National Research Foundation of Korea (NRF), which is funded by the Ministry of Education, Science and Technology (MEST) (No. 2009-00831530); and the research program for New Drug Target Discovery through the NRF of Korea, which is funded by the MEST (No. 2009-0093927). KH Jeong is a recipient of Seoul Science Fellowship and J Jeong was supported by the RCFC (R11-2005-009-03004-0).

Appendix A. Supplementary data

Supplementary data associated with this article can be found, in the online version, at doi:10.1016/j.ydbio.2010.06.004.

References

- Acquaviva, C., Herzog, F., Kraft, C., Pines, J., 2004. The anaphase promoting complex/cyclosome is recruited to centromeres by the spindle assembly checkpoint. *Cell Biol.* 6, 892–898.
- Archambault, V., Glover, D.M., 2009. Polo-like kinases: conservation and divergence in their functions and regulation. *Nat. Rev. Mol. Cell Biol.* 10, 265–275.
- Barr, F.A., Sillje, H.H., Nigg, E.A., 2004. Polo-like kinases and the orchestration of cell division. *Nat. Rev. Mol. Cell Biol.* 5, 429–440.
- Bettencourt-Dias, M., Rodrigues-Martins, A., Carpenter, L., Riparbelli, M., Lehmann, L., Gatt, M.K., Carmo, N., Balloux, F., Callaini, G., Glover, D.M., 2005. SAK/PLK4 is required for centriole duplication and flagella development. *Curr. Biol.* 15, 2199–2207.
- Budirahardja, Y., Gonczy, P., 2008. PLK-1 asymmetry contributes to asynchronous cell division of *C. elegans* embryos. *Development* 135, 1303–1313.
- Budirahardja, Y., Gonczy, P., 2009. Coupling the cell cycle to development. *Development* 136, 2861–2872.
- Cheng, K.Y., Lowe, E.D., Sinclair, J., Nigg, E.A., Johnson, L.N., 2003. The crystal structure of the human polo-like kinase-1 polo box domain and its phospho-peptide complex. *EMBO J.* 22, 5757–5768.
- Chi, Y.H., Haller, K., Ward, M.D., Semmes, O.J., Li, Y., Jeang, K.T., 2008. Requirements for protein phosphorylation and the kinase activity of polo-like kinase 1 (Plk1) for the kinetochore function of mitotic arrest deficiency protein 1 (Mad1). *J. Biol. Chem.*
- Choi, E., Choe, H., Min, J., Choi, J.Y., Kim, J., Lee, H., 2009. BubR1 acetylation at prometaphase is required for modulating APC/C activity and timing of mitosis. *EMBO J.* 28, 2077–2089.
- Chung, E., Chen, R.H., 2002. Spindle checkpoint requires Mad1-bound and Mad1-free Mad2. *Mol. Biol. Cell* 13, 1501–1511.
- Davis, F.M., Tsao, T.Y., Fowler, S.K., Rao, P.N., 1983. Monoclonal antibodies to mitotic cells. *Proc. Natl. Acad. Sci. U. S. A.* 80, 2926–2930.
- Elia, A.E., Cantley, L.C., Yaffe, M.B., 2003a. Proteomic screen finds pSer/pThr-binding domain localizing Plk1 to mitotic substrates. *Science* 299, 1228–1231.
- Elia, A.E., Rellos, P., Haire, L.F., Chao, J.W., Ivins, F.J., Hoepker, K., Mohammad, D., Cantley, L.C., Smerdon, S.J., Yaffe, M.B., 2003b. The molecular basis for phosphodependent substrate targeting and regulation of Plks by the Polo-box domain. *Cell* 115, 83–95.
- Elowe, S., Hummer, S., Ultschmid, A., Li, X., Nigg, E.A., 2007. Tension-sensitive Plk1 phosphorylation on BubR1 regulates the stability of kinetochore microtubule interactions. *Genes Dev.* 21, 2205–2219.
- Garcia-Alvarez, B., de Carcer, G., Ibanez, S., Bragado-Nilsson, E., Montoya, G., 2007. Molecular and structural basis of polo-like kinase 1 substrate recognition: implications in centrosomal localization. *Proc. Natl. Acad. Sci. U. S. A.* 104, 3107–3112.
- Ghosh, S., Paweletz, N., Schroeter, D., 1993. Failure of centromere separation leads to formation of diplochromosomes in next mitosis in okadaic acid treated HeLa cells. *Cell Biol. Int.* 17, 949–952.
- Giet, R., Glover, D.M., 2001. Drosophila aurora B kinase is required for histone H3 phosphorylation and condensin recruitment during chromosome condensation and to organize the central spindle during cytokinesis. *J. Cell Biol.* 152, 669–682.
- Gimenez-Abian, J.F., Sumara, I., Hirota, T., Hauf, S., Gerlich, D., de la Torre, C., Ellenberg, J., Peters, J.M., 2004. Regulation of sister chromatid cohesion between chromosome arms. *Curr. Biol.* 14, 1187–1193.
- Gisselsson, D., 2008. Classification of chromosome segregation errors in cancer. *Chromosoma* 117, 511–519.
- Goyanes, V.J., Schwartzman, J.B., 1981. Insights on diplochromosome structure and behaviour. *Chromosoma* 83, 93–102.
- Gumireddy, K., Reddy, M.V., Cosenza, S.C., Boominathan, R., Baker, S.J., Papathi, N., Jiang, J., Holland, J., Reddy, E.P., 2005. ONO1910, a non-ATP-competitive small molecule inhibitor of Plk1, is a potent anticancer agent. *Cancer Cell* 7, 275–286.
- Habedanck, R., Stierhof, Y.D., Wilkinson, C.J., Nigg, E.A., 2005. The Polo kinase Plk4 functions in centriole duplication. *Nat. Cell Biol.* 7, 1140–1146.
- Hagting, A., Den Elzen, N., Vodermaier, H.C., Waizenegger, I.C., Peters, J.M., Pines, J., 2002. Human securin proteolysis is controlled by the spindle checkpoint and reveals when the APC/C switches from activation by Cdc20 to Cdh1. *J. Cell Biol.* 157, 1125–1137.
- Hardwick, K.G., Murray, A.W., 1995. Mad1p, a phosphoprotein component of the spindle assembly checkpoint in budding yeast. *J. Cell Biol.* 131, 709–720.
- Hartwell, L.H., Smith, D., 1985. Altered fidelity of mitotic chromosome transmission in cell cycle mutants of *S. cerevisiae*. *Genetics* 110, 381–395.
- Hauf, S., Roitinger, E., Koch, B., Dittrich, C.M., Mechtler, K., Peters, J.M., 2005. Dissociation of cohesin from chromosome arms and loss of arm cohesion during early mitosis depends on phosphorylation of SA2. *PLoS Biol.* 3, e69.
- Hsu, J.Y., Sun, Z.W., Li, X., Reuben, M., Tatchell, K., Bishop, D.K., Grushcow, J.M., Brame, C. J., Caldwell, J.A., Hunt, D.F., Lin, R., Smith, M.M., Allis, C.D., 2000. Mitotic phosphorylation of histone H3 is governed by Ipl1/aurora kinase and Glc7/PP1 phosphatase in budding yeast and nematodes. *Cell* 102, 279–291.
- Jeong, J.Y., Einhorn, Z., Mercurio, S., Lee, S., Lau, B., Mione, M., Wilson, S.W., Guo, S., 2006. Neurogenin1 is a determinant of zebrafish basal forebrain dopaminergic neurons and is regulated by the conserved zinc finger protein Tof/Fez1. *Proc. Natl. Acad. Sci. U. S. A.* 103, 5143–5148.
- Kanda, T., Sullivan, K.F., Wahl, G.M., 1998. Histone-GFP fusion protein enables sensitive analysis of chromosome dynamics in living mammalian cells. *Curr. Biol.* 8, 377–385.
- Kang, Y.H., Park, J.E., Yu, L.R., Soung, N.K., Yun, S.M., Bang, J.K., Seong, Y.S., Yu, H., Garfield, S., Veenstra, T.D., Lee, K.S., 2006. Self-regulated Plk1 recruitment to kinetochores by the Plk1-PBIP1 interaction is critical for proper chromosome segregation. *Mol. Cell* 24, 409–422.
- Kimmel, C.B., Ballard, W.W., Kimmel, S.R., Ullmann, B., Schilling, T.F., 1995. Stages of embryonic development of the zebrafish. *Dev. Dyn.* 203, 253–310.
- Ko, M.A., Rosario, C.O., Hudson, J.W., Kulkarni, S., Pollett, A., Dennis, J.W., Swallow, C.J., 2005. Plk4 haploinsufficiency causes mitotic infidelity and carcinogenesis. *Nat. Genet.* 37, 883–888.
- Kumada, K., Yao, R., Kawaguchi, T., Karasawa, M., Hoshikawa, Y., Ichikawa, K., Sugitani, Y., Imoto, I., Inazawa, J., Sugawara, M., Yanagida, M., Noda, T., 2006. The selective continued linkage of centromeres from mitosis to interphase in the absence of mammalian separase. *J. Cell Biol.* 172, 835–846.
- Lane, H.A., Nigg, E.A., 1996. Antibody microinjection reveals an essential role for human polo-like kinase 1 (Plk1) in the functional maturation of mitotic centrosomes. *J. Cell Biol.* 135, 1701–1713.
- Lee, H., Kimelman, D., 2002. A dominant-negative form of p63 is required for epidermal proliferation in zebrafish. *Dev. Cell* 2, 607–616.
- Lee, K.S., Grenfell, T.Z., Yarm, F.R., Erikson, R.L., 1998. Mutation of the polo-box disrupts localization and mitotic functions of the mammalian polo kinase Plk. *Proc. Natl. Acad. Sci. U. S. A.* 95, 9301–9306.
- Lee, H., Trainer, A.H., Friedman, L.S., Thistlethwaite, F.C., Evans, M.J., Ponder, B.A., Venkitaraman, A.R., 1999. Mitotic checkpoint inactivation fosters transformation in cells lacking the breast cancer susceptibility gene, *Bra2*. *Mol. Cell* 4, 1–10.
- Lee, K.S., Park, J.E., Asano, S., Park, C.J., 2005. Yeast polo-like kinases: functionally conserved multitask mitotic regulators. *Oncogene* 24, 217–229.
- Lenart, P., Petronczki, M., Stegmaier, M., Di Fiore, B., Lipp, J.J., Hoffmann, M., Rettig, W.J., Kraut, N., Peters, J.M., 2007. The small-molecule inhibitor BI 2536 reveals novel insights into mitotic roles of polo-like kinase 1. *Curr. Biol.* 17, 304–315.

- Lindon, C., Pines, J., 2004. Ordered proteolysis in anaphase inactivates Plk1 to contribute to proper mitotic exit in human cells. *J. Cell Biol.* 164, 233–241.
- Liu, X., Lei, M., Erikson, R.L., 2006. Normal cells, but not cancer cells, survive severe Plk1 depletion. *Mol. Cell Biol.* 26, 2093–2108.
- Llamazares, S., Moreira, A., Tavares, A., Girdham, C., Spruce, B.A., Gonzalez, C., Karess, R. E., Glover, D.M., Sunkel, C.E., 1991. polo encodes a protein kinase homolog required for mitosis in *Drosophila*. *Genes Dev.* 5, 2153–2165.
- Losada, A., Hirano, M., Hirano, T., 2002. Cohesin release is required for sister chromatid resolution, but not for condensin-mediated compaction, at the onset of mitosis. *Genes Dev.* 16, 3004–3016.
- Lu, L.Y., Wood, J.L., Minter-Dykhouse, K., Ye, L., Saunders, T.L., Yu, X., Chen, J., 2008. Polo-like kinase 1 is essential for early embryonic development and tumor suppression. *Mol. Cell Biol.* 28, 6870–6876.
- Mundt, K.E., Golsteyn, R.M., Lane, H.A., Nigg, E.A., 1997. On the regulation and function of human polo-like kinase 1 (PLK1): effects of overexpression on cell cycle progression. *Biochem. Biophys. Res. Commun.* 239, 377–385.
- Nasmyth, K., 2002. Segregating sister genomes: the molecular biology of chromosome separation. *Science* 297, 559–565.
- Nasmyth, K., 2005. How do so few control so many? *Cell* 120, 739–746.
- Nasmyth, K., Haering, C.H., 2009. Cohesin: its roles and mechanisms. *Annu. Rev. Genet.* 43, 525–558.
- Nilsson, J., Yekezare, M., Minshull, J., Pines, J., 2008. The APC/C maintains the spindle assembly checkpoint by targeting Cdc20 for destruction. *Nat. Cell Biol.*
- Ohkura, H., Hagan, I.M., Glover, D.M., 1995. The conserved *Schizosaccharomyces pombe* kinase plo1, required to form a bipolar spindle, the actin ring, and septum, can drive septum formation in G1 and G2 cells. *Genes Dev.* 9, 1059–1073.
- Peters, J.M., 2006. The anaphase promoting complex/cyclosome: a machine designed to destroy. *Nat. Rev. Mol. Cell Biol.* 7, 644–656.
- Peters, J.M., Tedeschi, A., Schmitz, J., 2008. The cohesin complex and its roles in chromosome biology. *Genes Dev.* 22, 3089–3114.
- Petronczki, M., Lenart, P., Peters, J.M., 2008. Polo on the rise—from mitotic entry to cytokinesis with Plk1. *Dev. Cell* 14, 646–659.
- Qian, Y.W., Erikson, E., Li, C., Maller, J.L., 1998. Activated polo-like kinase Plx1 is required at multiple points during mitosis in *Xenopus laevis*. *Mol. Cell Biol.* 18, 4262–4271.
- Qian, Y.W., Erikson, E., Taieb, F.E., Maller, J.L., 2001. The polo-like kinase Plx1 is required for activation of the phosphatase Cdc25C and cyclin B-Cdc2 in *Xenopus* oocytes. *Mol. Biol. Cell* 12, 1791–1799.
- Rivers, D.M., Moreno, S., Abraham, M., Ahringer, J., 2008. PAR proteins direct asymmetry of the cell cycle regulators Polo-like kinase and Cdc25. *J. Cell Biol.* 180, 877–885.
- Shepard, J.L., Amatruda, J.F., Stern, H.M., Subramanian, A., Finkelstein, D., Ziai, J., Finley, K.R., Pfaff, K.L., Hersey, C., Zhou, Y., Barut, B., Freedman, M., Lee, C., Spitsbergen, J., Neuberg, D., Weber, G., Golub, T.R., Glickman, J.N., Kutok, J.L., Aster, J.C., Zon, L.I., 2005. A zebrafish myb mutation causes genome instability and increased cancer susceptibility. *Proc. Natl. Acad. Sci. U. S. A.* 102, 13194–13199.
- Shepard, J.L., Amatruda, J.F., Finkelstein, D., Ziai, J., Finley, K.R., Stern, H.M., Chiang, K., Hersey, C., Barut, B., Freeman, J.L., Lee, C., Glickman, J.N., Kutok, J.L., Aster, J.C., Zon, L. I., 2007. A mutation in separase causes genome instability and increased susceptibility to epithelial cancer. *Genes Dev.* 21, 55–59.
- Sironi, L., Melixetian, M., Faretta, M., Prosperini, E., Helin, K., Musacchio, A., 2001. Mad2 binding to Mad1 and Cdc20, rather than oligomerization, is required for the spindle checkpoint. *EMBO J.* 20, 6371–6382.
- Smith, M.R., Wilson, M.L., Hamanaka, R., Chase, D., Kung, H., Longo, D.L., Ferris, D.K., 1997. Malignant transformation of mammalian cells initiated by constitutive expression of the polo-like kinase. *Biochem. Biophys. Res. Commun.* 234, 397–405.
- Steggmaier, M., Hoffmann, M., Baum, A., Lenart, P., Petronczki, M., Krssak, M., Gurtler, U., Garin-Chesa, P., Lieb, S., Quant, J., Grauert, M., Adolf, G.R., Kraut, N., Peters, J.M., Rettig, W.J., 2007. BI 2536, a potent and selective inhibitor of polo-like kinase 1, inhibits tumor growth in vivo. *Curr. Biol.* 17, 316–322.
- Stratmann, R., Lehner, C.F., 1996. Separation of sister chromatids in mitosis requires the *Drosophila* pimpls product, a protein degraded after the metaphase/anaphase transition. *Cell* 84, 25–35.
- Sumara, I., Vorlaufer, E., Stukenberg, P.T., Kelm, O., Redemann, N., Nigg, E.A., Peters, J.M., 2002. The dissociation of cohesin from chromosomes in prophase is regulated by Polo-like kinase. *Mol. Cell* 9, 515–525.
- Sunkel, C.E., Glover, D.M., 1988. polo, a mitotic mutant of *Drosophila* displaying abnormal spindle poles. *J. Cell Sci.* 89 (Pt 1), 25–38.
- Takai, N., Hamanaka, R., Yoshimatsu, J., Miyakawa, I., 2005. Polo-like kinases (Plks) and cancer. *Oncogene* 24, 287–291.
- Tang, J., Erikson, R.L., Liu, X., 2006. Ectopic expression of Plk1 leads to activation of the spindle checkpoint. *Cell Cycle* 5, 2484–2488.
- Taylor, S., Peters, J.M., 2008. Polo and Aurora kinases: lessons derived from chemical biology. *Curr. Opin. Cell Biol.* 20, 77–84.
- Urasaki, A., Morvan, G., Kawakami, K., 2006. Functional dissection of the Tol2 transposable element identified the minimal cis-sequence and a highly repetitive sequence in the subterminal region essential for transposition. *Genetics* 174, 639–649.
- van de Weerd, B.C., Littler, D.R., Klompaker, R., Huseinovic, A., Fish, A., Perrakis, A., Medema, R.H., 2008. Polo-box domains confer target specificity to the Polo-like kinase family. *Biochim. Biophys. Acta* 1783, 1015–1022.
- Watanabe, Y., Kitajima, T.S., 2005. Shugoshin protects cohesin complexes at centromeres. *Philos. Trans. R. Soc. Lond. B Biol. Sci.* 360, 515–521 (discussion 521).